ACS OMEGA

http://pubs.acs.org/journal/acsodf

Article

Thermoelectric Properties of Pristine Graphyne and the BN-Doped Graphyne Family

Jyotirmoy Deb, Rajkumar Mondal, Utpal Sarkar,* and Hatef Sadeghi*

Cite This: *ACS Omega* 2021, 6, 20149−20157

Read Online

ACCESS | Metrics & More | Article Recommendations | Supporting Information

ABSTRACT: In this paper, we have investigated the thermoelectric properties of BN-doped graphynes and compared them with respect to their pristine counterpart using first-principles calculations. The effect of temperature on the thermoelectric properties has also been explored. Pristine γ-graphyne is an intrinsic band gap semiconductor and the band gap significantly increases due to the incorporation of boron and nitrogen atoms into the system, which simultaneously results in high electrical conductivity, a large Seebeck coefficient, and low thermal conductivity. The Seebeck coefficient for all these systems is significantly higher than that of conventional thermoelectric materials, suggesting their potential in thermoelectric applications. Among all the considered systems, the "graphyne-like BN sheet" has the highest electrical conductance and lowest thermal conductance, ensuring its superiority in thermoelectric properties over the other studied systems. We find that a maximum full ZT of ∼6 at room temperature is accessible in the "graphyne-like BN sheet".

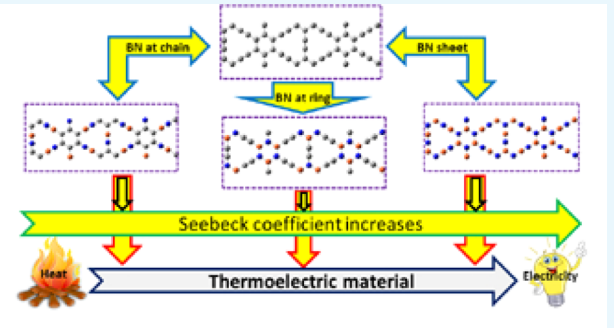

Thermoelectric performance of BN-doped graphyne family

INTRODUCTION

The rapid advancement of human civilization during recent days demands a huge energy requirement, which is not able to be fulfilled from the natural resources available and thus leads to the global energy crisis. To overcome this crisis, various ways have been adopted, among which thermoelectric energy conversion plays a very vital role and is an essential requirement for fulfilling the demand for next-generation nanoelectronic devices.[1] Thermoelectric technology is one of the most effective methods for energy harvesting since it provides a pavement that can convert waste heat into electricity and *vice versa*. That is why thermoelectric materials have gained significant attention among the research community during the present days.[1,2] The performance of a thermoelectric material is characterized by a dimensionless quantity, namely, the figure of merit[3] ZT and is defined as $ZT = \frac{GS^2T}{k_e + k_{ph}}$, where G is the electrical conductance, S is the Seebeck coefficient, T is the temperature, k_e is the electronic part of thermal conductance, and k_{ph} is the phonon contribution of thermal conductance. To achieve a high ZT, a thermoelectric material should possess a large Seebeck coefficient and electrical conductance (a high value of power factor S^2G) and simultaneously a low thermal conductance. In general, it is difficult to fulfill the above criteria as all these transport coefficients S, G, and k are coupled with each other in traditional thermoelectric materials. However, recent studies show that low-dimensional systems can possess a high ZT due to the quantum confinement effect.[4,5] Thus, searching for low-dimensional nanomaterials with high thermoelectric efficiency is becoming a challenging task for the research community. Literature survey reveals that a carbon-based material is a great choice for designing and fabricating efficient thermoelectric materials.[6−13] Among these carbon-based materials, graphene[14] finds vast applications[15,16] but the presence of zero band gap results in a very small Seebeck coefficient of graphene along with high thermal conductivity, which significantly reduces its thermoelectric performance.[17] To reduce its thermal conductance, enormous efforts have been put in such as defect engineering,[18,19] isotope engineering,[20] and a superlattice structure.[21] Another two-dimensional (2D) carbon allotrope, namely, graphyne,[22] is formed by inserting acetylenic linkages (sp hybridization) in between two carbon atoms of graphene. By varying the number and position of acetylenic linkages, several substructures of graphyne can be obtained such as α-, β-, γ-, 6,6,12-graphyne, and graphdiyne.[23,24] Among these, α-, β-, and 6,6,12-graphyne show characteristics of a Dirac material while γ-graphyne and graphdiyne are intrinsic semiconductors in nature.[24] The presence of versatile characteristics in γ-graphyne makes it a suitable candidate for

Received: March 23, 2021
Accepted: July 21, 2021
Published: July 28, 2021

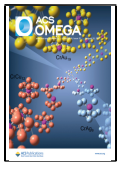

electronic,[25,26] optoelectronic,[27−29] gas sensing,[30,31] energy storage,[32] and spintronic devices.[33] The presence of a band gap also leads to a significant enhancement of its Seebeck coefficient[13] and the presence of acetylenic linkages reduces the thermal conductivity significantly.[13] All these surveys prompt that γ-graphyne is a promising candidate for a future thermoelectric material, as already reported by several researchers theoretically.[10,11,13] Recent advances in experimental synthesis of γ-graphyne[34] open a new door for fabrication of thermoelectric devices based on graphyne. As the band gap is responsible for the large Seebeck coefficient, the thermoelectric performance of graphyne can be tuned by engineering its band gap. One of the effective methods for tuning the band gap is doping with suitable atoms. Interestingly, it has been observed that the band gap of γ-graphyne can be increased by co-doping with B and N atoms at different positions.[28,29,35,36]

Motivated by the above findings, here for the first time, we investigate the thermoelectric properties of BN-doped γ-graphynes and compare its performance with its pristine counterpart. Interestingly, it has been observed that doping with the B or N atom increases the band gap, thus leading to a large Seebeck coefficient and high thermoelectric performance of BN-doped γ-graphynes compared to pristine γ-graphyne. Incorporating B and N atoms in other systems such as holey graphene, graphene oxide, and so forth significantly enhances the thermoelectric performance,[37,38] which is another reason for choosing B and N atoms as dopants in our present study. For any thermoelectric device, p-type and n-type materials need to be arranged in a tandem device to increase its thermal voltage output. This is achieved in our study by co-doping with B and N atoms.[39]

COMPUTATIONAL METHODOLOGY

To obtain the optimized geometry and ground-state Hamiltonian of all these materials, we have used SIESTA 3.2 computational package[40] using density functional theory (DFT). The Perdew−Burke−Ernzerhof method[41] is used to account for the exchange and correlation functional of generalized gradient approximation. Troullier−Martins-type norm-conserving pseudopotentials[42] are used to account for the core electrons and linear combinations of atomic orbitals to construct the valence states. A double-ζ-plus polarized numerical atomic orbitals type basis set along with a real-space grid having a mesh cut-off energy of 600 Ry is considered for the calculation. The Brillouin zone is sampled using a 1 × 12 × 12 Monkhorst−Pack grid k-point, and a maximum force tolerance of 0.01 eV/Å is used in the calculation. A vacuum of 15 Å is kept along X-direction to avoid the interaction between two periodic images.

Transport Calculation. The mean-field Hamiltonians obtained from the converged DFT calculations are combined with the quantum transport code GOLLUM.[43,44] The transmission coefficient, $T(E)$, for electrons passing from the source to the drain with energy E is calculated through the relation

$$T(E) = \mathrm{trace}\{\Gamma_R(E)G^R(E)\Gamma_L(E)G^{R\dagger}(E)\} \quad (1)$$

where $\Gamma_{L,R}(E) = i[\Sigma_{L,R}(E) - \Sigma^{\dagger}_{L,R}(E)]$ describes the broadening due to the coupling between the central scattering region (SR) and left (L) and right (R) electrodes. $\Sigma_{L,R}(E)$ are the retarded self-energies associated with this coupling. $G^R = (ES - H - \Sigma_L - \Sigma_R)^{-1}$ is the retarded Green's function where H is the Hamiltonian and S is the overlap matrix.

Thermoelectric properties such as the electrical conductance (G), Seebeck coefficient (S), and electronic part of thermal conductance (k_e) of the device as a function of temperature are calculated using the following relations[43,45]

$$G(E_F, T) = G_0 L_0 \quad (2)$$

$$k_e(E_F, T) = \frac{L_0 L_2 - L_1^2}{hTL_0} \quad (3)$$

$$S(E_F, T) = -\frac{L_1}{eTL_0} \quad (4)$$

$$L_n(E_F, T) = \int_{-\infty}^{+\infty} dE(E - E_F)^n T(E)\left(-\frac{\partial f(E)}{\partial E}\right) \quad (5)$$

where $f(E)$ is the Fermi−Dirac probability distribution function, T is the temperature, E_F is the Fermi energy, $G_0 = 2e^2/h$ is the quantum conductance, e is the charge of the electron, and h is Planck's constant.

After obtaining the transmission as a function of energy $[T(E)]$, we have calculated the integral $L_n(E_F, T)$ using eq 5. This equation depends on temperature and Fermi energy. To calculate the electrical conductance $G(E_F, T)$, we use the Landauer formula as given in eq 2 where the term L_0 is obtained from eq 5. We then calculate G versus the Fermi energy for fixed temperatures as shown in Figure 4. The other thermoelectric parameters such as the Seebeck coefficient (S) and electronic part of thermal conductance (k_e) also depend on the integral $L_n(E_F, T)$ and can be calculated using the relations 3 and 4.

It is worth mentioning that we calculate the thermoelectric properties of structures under the assumption that the charge state of the structures and their electronic structure are not changed by changes of Fermi energy (E_F) or temperature (T), which is valid for small changes in E_F and T.

RESULTS AND DISCUSSION

In this work, we have studied the thermoelectric properties of 2D BN-doped γ-graphynes and compared them with pristine γ-graphyne. For BN-doped systems, we have considered three configurations as "γ-graphyne with BN at the hexagonal ring", "γ-graphyne with BN at the chain" and "γ-graphyne-like BN sheet". The device comprising the SR sandwiched between two electrodes is presented in Figure 1 and the corresponding coordinates of the structures are provided in Table S1 of the Supporting Information. State-of-the-art theoretical calculations by several research groups already confirmed the stability of the above-mentioned systems.[28,35,36,46,47] Thus, we considered pristine γ-graphyne and its BN-derivatives for making the device.

We then calculate the thermoelectric properties such as Seebeck coefficients, the electronic contribution to the thermal conductance, and the electronic part of figure of merit for pristine and BN-doped γ-graphyne and discuss their variation with temperatures. All of these parameters are obtained from the energy dependence of the electron transmission coefficient.

Figure 2 shows the electron transmission spectra $[T(E)]$ at zero bias voltage as a function of E within the energy range $[-3.0, +3.0]$ eV. There is an energy band gap in all transmissions that follows "pristine γ-graphyne" < "γ-graphyne

https://doi.org/10.1021/acsomega.1c01538
ACS Omega 2021, 6, 20149−20157

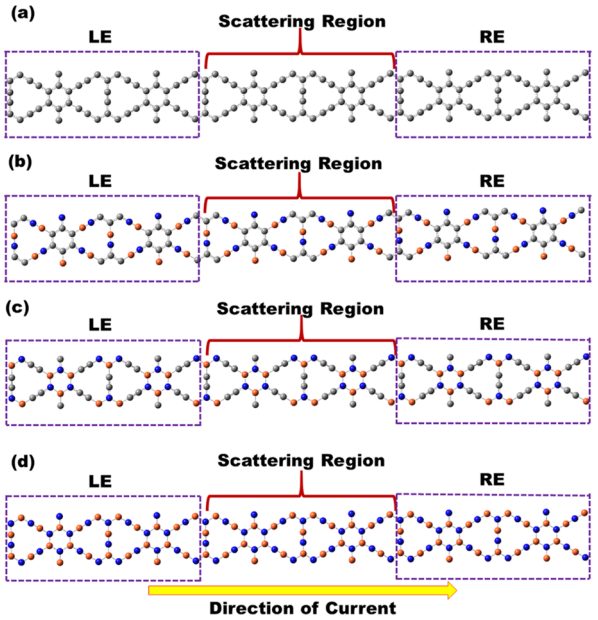

Figure 1. Representative device model showing two electrodes and the SR (a) for pristine γ-graphyne nanojunction; (b) for γ-graphyne nanojunction with BN at the linear chain; (c) for the γ-graphyne nanojunction with BN at the hexagonal ring (d) for γ-graphyne-like BN sheet nanojunction. LE and RE represent the left electrode and right electrode, respectively.

with BN at the chain" < "γ-graphyne with BN at the hexagonal ring" < "γ-graphyne-like BN sheet".[35] The transmission spectra equal to the number of open channels and show stepwise behavior.

Figure 3 depicts the variation of the Seebeck coefficient (S) for the pristine and BN-doped γ-graphyne systems with Fermi energy at different temperatures (200, 300, and 500 K). The temperature gradient in a material initiates the flow of current between hot and cold electrodes and as a result, an electric field is developed across the two ends and hence a voltage, known as the Seebeck voltage. As observed in Figure 3a, the highest value of S is 1.01×10^{-3} V/K at 200 K (Table 1), corresponding to $E_F = \pm 0.03$ eV, which is much higher than that of a conventional thermoelectric material.[48] The S value decreases with an increase in temperature. The magnitude of S for pristine γ-graphyne at room temperature is 0.64×10^{-3} V/K (Table 1) and is in good agreement with the previously reported result[11] and the magnitude of S at room temperature is also much higher than that of the conventional thermoelectric material such as Bi_2Te_3.[48] Now for γ-graphyne with BN at the chain position, the highest value of S is 3.07×10^{-3} V/K (Table 1) at 200 K and the maximum values of S are found at the Fermi energy of −0.32 and +0.05 eV, respectively (Figure 3c). When BN is at the ring position of γ-graphyne, the highest value of S is 3.09×10^{-3} V/K at $T = 300$ K (Table 1) and the maximum value of S is recorded corresponding to the Fermi energy of −0.64 and +0.02 eV, respectively (Figure 3b). Finally, for the "γ-graphyne-like BN sheet", the maximum value of S is found at the Fermi energy +0.18 and +1.17 eV (Figure

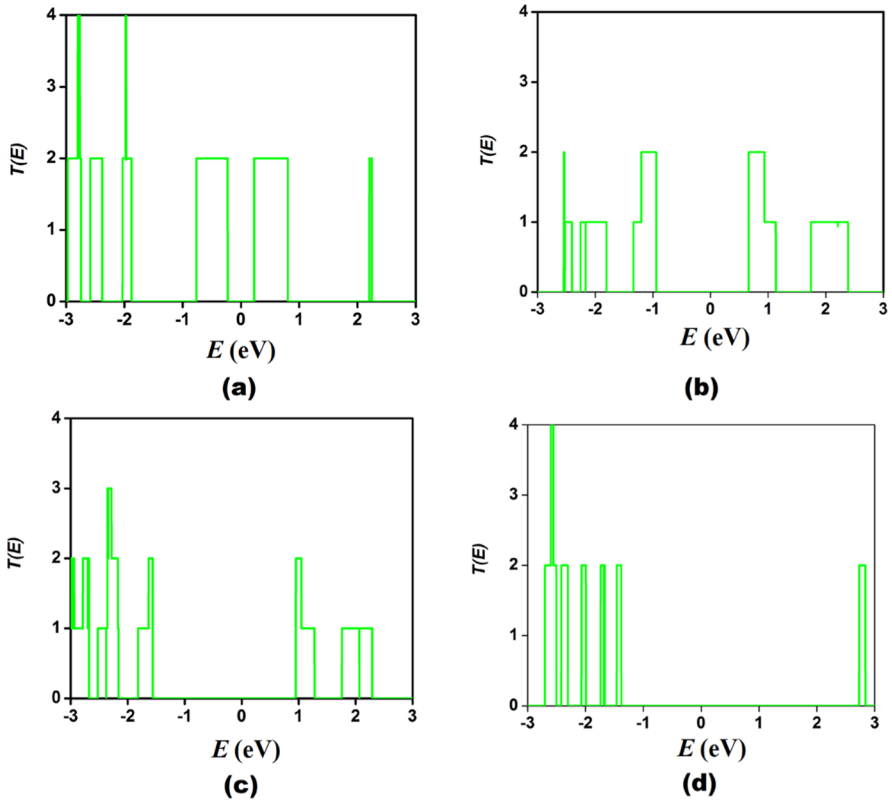

Figure 2. Variation of zero-bias transmission spectra with energy for (a) pristine γ-graphyne; (b) γ-graphyne with BN at linear chain; (c) γ-graphyne with BN at hexagonal ring; and (d) γ-graphyne-like BN sheet. $T(E)$ describes the transmission probability of electrons with energy E traversing from one side of the device to the other side. This is combined with eq 5 to calculate temperature-dependent quantities such as the conductance and the Seebeck coefficient (see the Computational Methodology section).

https://doi.org/10.1021/acsomega.1c01538
ACS Omega 2021, 6, 20149−20157

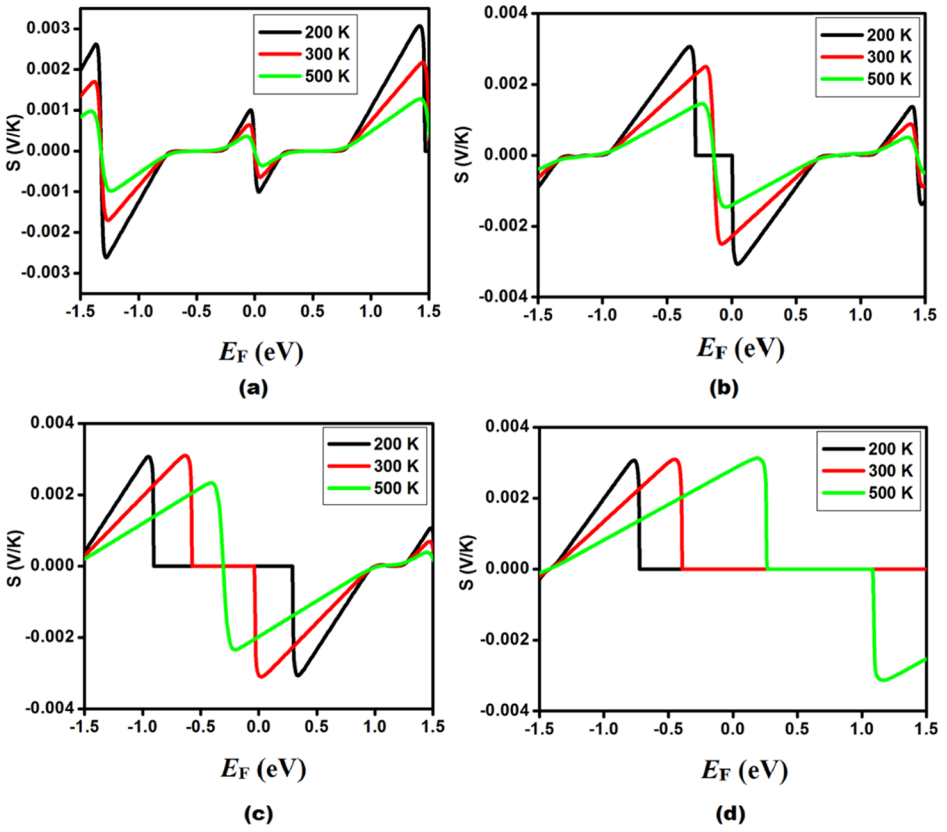

Figure 3. Variation of the Seebeck coefficient with Fermi energy for (a) pristine γ-graphyne; (b) γ-graphyne with BN at the linear chain; (c) γ-graphyne with BN at the hexagonal ring; and (d) γ-graphyne-like BN sheet at different temperatures.

Table 1. Calculated Seebeck Coefficient for Pristine and BN-Doped γ-Graphynes at Different Temperatures

system	T (K)	E_F (eV)	S (V/K)
pristine γ-graphyne	200	−0.03	1.01×10^{-3}
		0.03	-1.01×10^{-3}
	300	−0.05	0.64×10^{-3}
		0.05	-0.64×10^{-3}
	500	−0.07	0.36×10^{-3}
		0.07	-0.36×10^{-3}
γ-graphyne with BN at the chain	200	−0.32	3.07×10^{-3}
		0.05	-3.07×10^{-3}
	300	−0.20	2.50×10^{-3}
		−0.08	-2.50×10^{-3}
	500	−0.23	1.46×10^{-3}
		−0.05	-1.46×10^{-3}
γ-graphyne with BN at the ring	200	−0.95	3.07×10^{-3}
		0.33	-3.07×10^{-3}
	300	−0.64	3.09×10^{-3}
		0.02	-3.09×10^{-3}
	500	−0.41	2.33×10^{-3}
		−0.20	-2.34×10^{-3}
γ-graphyne-like BN sheet	200	−0.77	3.07×10^{-3}
		2.12	-3.07×10^{-3}
	300	−0.45	3.10×10^{-3}
		1.80	-3.10×10^{-3}
	500	0.18	3.13×10^{-3}
		1.17	-3.13×10^{-3}

3d) and the highest value of S is 3.13×10^{-3} V/K (Table 1). Interestingly, for the "γ-graphyne-like BN sheet" as the temperature increases, the asymmetric energy distribution of electrons around the Fermi level also increases, which leads to an increase in the magnitude of S with the temperature rise. The Seebeck coefficient of pristine γ-graphyne possess two peak values around the Fermi level irrespective of temperature and both of them have nearly the same value, indicating the isotropic nature of S. Although the magnitude of the two peaks is the same for BN-doped systems, for "γ-graphyne with BN at the chain" (at 300 and 500 K) and "γ-graphyne with BN at the ring" (at 500 K), both the peaks move toward the negative energy side, whereas the peaks shift toward the positive energy side for the "γ-graphyne-like BN sheet" (at 500 K) with respect to pristine γ-graphyne. This asymmetric energy distribution of electrons around the Fermi level for BN-doped systems leads to a greater value of the Seebeck coefficient. A system with a wide band gap generally has a large S value as S is related to E_g *via* the relation $S \approx -\left(\frac{k_B}{e}\right)\left(\frac{E_g}{2k_BT} + 2\right)$.[49] The wide band gap of pristine γ-graphyne, which is already reported by various groups,[25,35] contributes to the significant S value in this system. For pristine γ-graphyne, the calculated S value is higher than graphene[50] due to its semiconducting nature.[13] When BN has doped, the magnitude of S increases significantly compared to that of pristine γ-graphyne. The magnitudes of S at 300 and 500 K for all these systems increase in the following manner "pristine γ-graphyne" < "γ-graphyne with BN at the chain" < "γ-graphyne with BN at the ring" < "γ-graphyne-like BN sheet". This result is supported by the band gap characteristic of these systems. The Seebeck coefficient for all systems studied is significantly higher than for some other reported materials such as the boron arsenide sheet,[51] graphdiyne,[52] phosphorene,[53] $MoSe_2$,[54] WSe_2,[54] monolayer bismuth,[55] 1L-$ZnPSe_3$,[56]

https://doi.org/10.1021/acsomega.1c01538
ACS Omega 2021, 6, 20149−20157

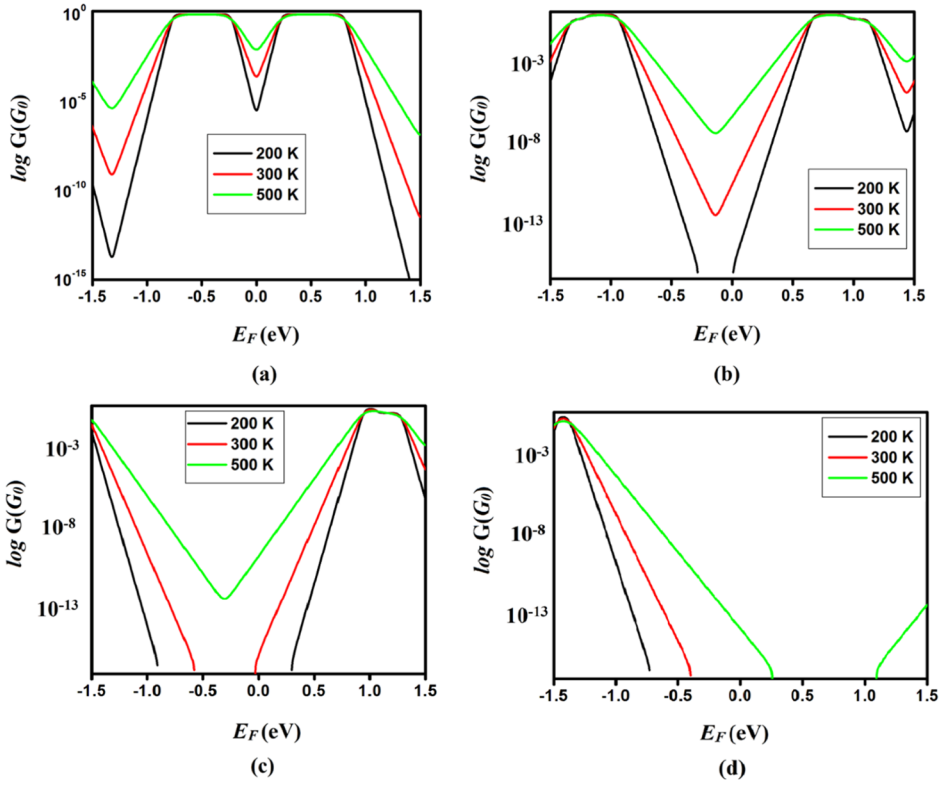

Figure 4. Variation of electrical conductance with Fermi energy for (a) pristine γ-graphyne; (b) γ-graphyne with BN at the linear chain; (c) γ-graphyne with BN at the hexagonal ring; and (d) γ-graphyne-like BN sheet at different temperatures.

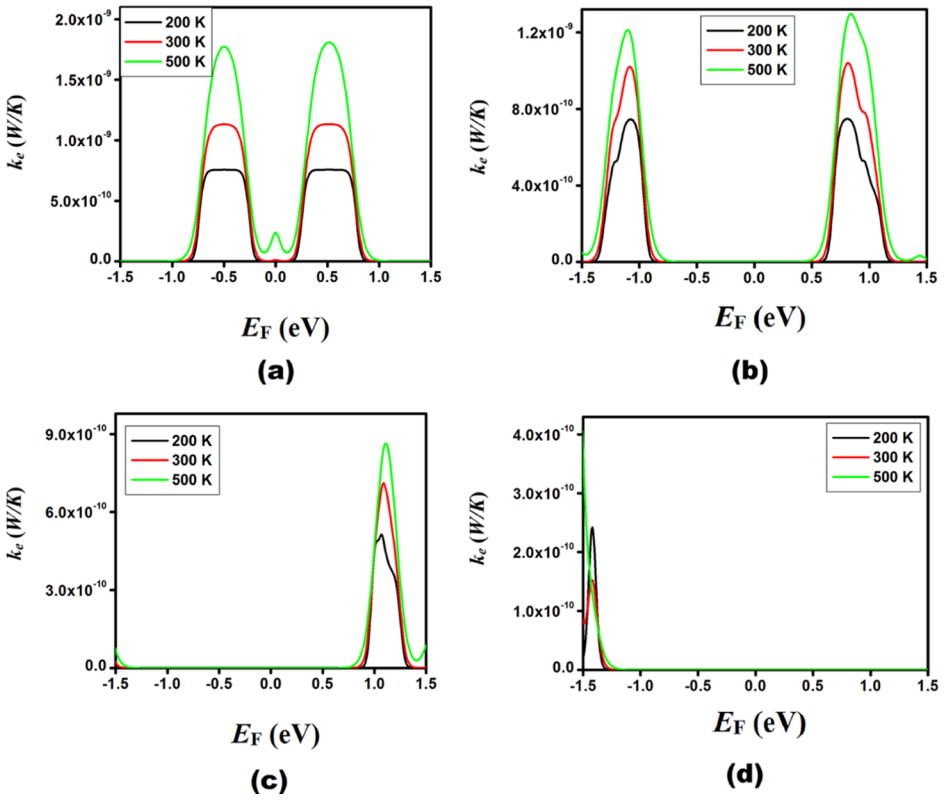

Figure 5. Variation of the electronic part of thermal conductance with Fermi energy for (a) pristine γ-graphyne; (b) γ-graphyne with BN at the linear chain; (c) γ-graphyne with BN at the hexagonal ring; and (d) γ-graphyne-like BN sheet at different temperatures.

selenene, and tellurene.[57] The experimental and theoretical studies already confirmed that a material to be used in thermoelectricity should have thermoelectric conversion performances of around 230 μV/K[58] and as all our studied

https://doi.org/10.1021/acsomega.1c01538
ACS Omega 2021, 6, 20149−20157

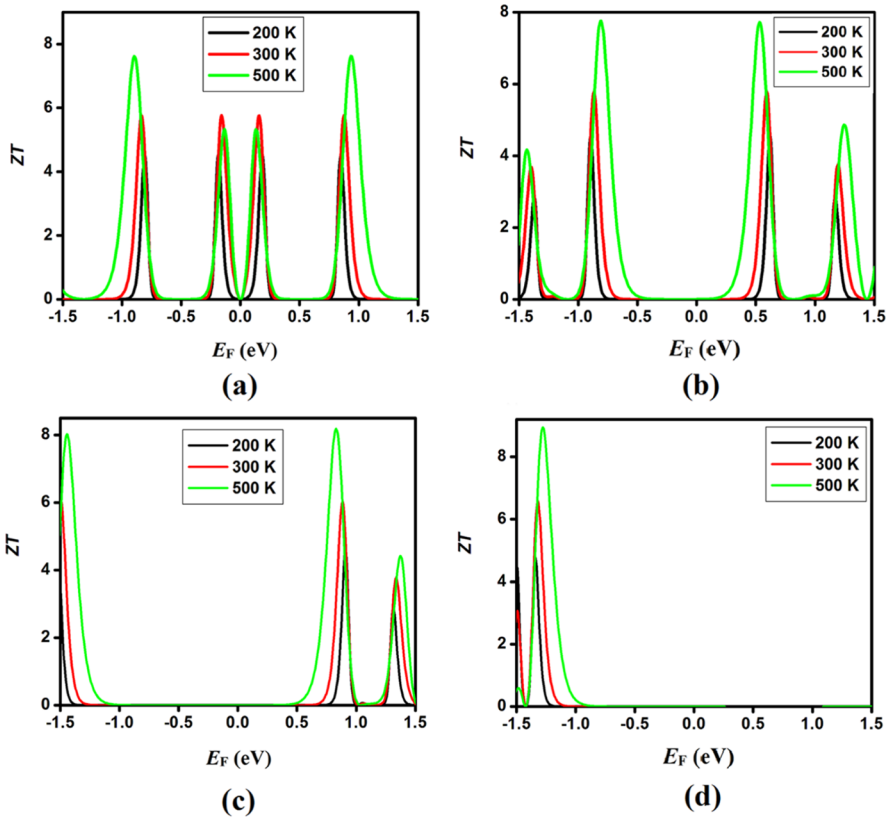

Figure 6. Variation of the figure of merit with Fermi energy for (a) pristine γ-graphyne; (b) γ-graphyne with BN at the linear chain; (c) γ-graphyne with BN at the hexagonal ring; and (d) γ-graphyne-like BN sheet at different temperatures.

material exhibits, a much higher Seebeck coefficient compared to the usual value, clearly suggesting the possibility of using these materials in thermoelectric applications. We found that the Seebeck coefficient is generally high in the structures studied. This is due to sharp features in the transmission functions. It is because the Seebeck coefficient is proportional to the slope of the transmission coefficient[59] $T(E)$ as $S \propto -\partial L_n T(E)/\partial E$ at E_F. This means that a flat transmission gives a zero Seebeck coefficient, while zones with large slopes give a high S. Furthermore, the sign of S changes for zones with positive and negative slopes. For example, the sign of S for pristine γ-graphyne is positive (negative) for energies around −0.2 eV (0.2 eV).

For a material to be applicable in thermoelectric applications, in addition to a high value of the Seebeck coefficient, a large magnitude of electrical conductance (G) is also needed. The electrical conductance (Figure 4) is highest for the "γ-graphyne-like BN sheet" and the magnitude is lowest for the "γ-graphyne with BN at the ring". The magnitude of G increases with temperature in the gap (*e.g.*, E = [−0.2 to +0.2]); however, it decreases on resonances (*e.g.*, E = [−0.8 to +0.4]) for all these systems. However, for the "γ-graphyne-like BN sheet", the decrement in G is more prominent compared to the rest of the systems.

The electronic part of thermal conductance is small for all these materials (Figure 5). The highest k_e is observed for pristine γ-graphyne while k_e is lowest for the "γ-graphyne-like BN sheet". The magnitude of k_e increases with an increase in T. The thermal conductance shows a similar trend with the electrical conductance in agreement with the Wiedemann–Franz law.

After obtaining all the transport coefficients, we have finally calculated the electronic thermoelectric figure of merit of pristine and BN-doped γ-graphyne systems using the relation $ZT_e = \frac{GS^2T}{k_e}$. Here, we have considered only the electronic part of the figure of merit. Figure S1 shows the variation of ZT_e as a function of the Fermi energy for different temperatures. For all these systems, two obvious peaks around the Fermi level have been observed. ZT_e for "pristine γ-graphyne" and "γ-graphyne with BN at the chain" decreases with an increase in temperature, while for "γ-graphyne with BN at the ring" it increases first (200 to 300 K) and then decreases (300 to 500 K) (Table S2). In the case of the "γ-graphyne-like BN sheet", ZT_e increases with an increase in temperature and it also has the highest ZT_e among the considered systems. The phonon thermal conductivity of pristine γ-graphyne is predicted to be about 75 W/mK at room temperature.[11] From this, we estimate the phonon contribution to thermal conductance in our pristine γ-graphyne junction as k_{ph} = 30 pW/K. Using this value, the full $ZT = ZT_e/(1 + k_{ph}/k_e)$ is obtained for the pristine γ-graphyne junction as shown in Figure 6a. Phonon band structure of these systems calculated using first-principles methods including all phonon modes are shown in Figure S2 of the Supporting Information. This indicates that they a have similar dispersion relation. The Debye frequency of "pristine γ-graphyne" is amongst the highest. It is expected that it should have higher thermal conductance (k_{ph}) than the "γ-graphyne-like BN sheet" and "γ-graphyne with BN at the chain". Its thermal conductance (k_{ph}) also should be close to the k_{ph} of "γ-graphyne with BN at the hexagonal ring", especially the small difference in Debye frequency happens to be in high

https://doi.org/10.1021/acsomega.1c01538
ACS Omega 2021, 6, 20149−20157

frequencies with a small contribution to room temperature k_{ph}. Figure 6 shows the estimated full ZT. Clearly, ZT is high in these materials. This is an indication that these systems hold great potential for thermoelectricity. Among all the considered systems, the "γ-graphyne-like BN sheet" possesses the highest maximum ZT and a maximum ZT of ∼6 is observed at room temperature. This is the minimum ZT expected as the Debye frequency of the "γ-graphyne-like BN sheet" is lower than that of "pristine γ-graphyne", and k_{ph} for the "γ-graphyne-like BN sheet" is expected to be lower than that used to estimate the full ZT and therefore full ZT is expected to be higher than these values. The other factors which attribute to the highest ZT in the "γ-graphyne-like BN sheet" are the largest Seebeck coefficient (S), largest electrical conductance (G), and lowest electrical thermal conductance (k_e) of the "γ-graphyne-like BN sheet" compared to other systems.

A previous study[60] by our group shows that a double vacancy in γ-graphyne results in a wide band gap semiconductor with a band gap of 1.82 eV for majority spin while the band gap for minority spin is 1.34 eV. This wide band gap indicates that double vacancy in γ-graphyne will lead to a large Seebeck coefficient. Literature survey also reveals that the introduction of the defective environment in the γ-graphyne nanoribbon system significantly enhances the thermoelectric performance of the material.[61−63] Therefore, we expect further enhancement with defects in our structures too.

CONCLUSIONS

In conclusion, within the framework of DFT in association with the quantum transport technique, the thermoelectric properties of BN-doped γ-graphynes with varying temperatures have been investigated and compared with respect to their pristine analogue. The Seebeck coefficient of all these doped systems is significantly higher than those of conventional thermoelectric materials, ensuring their potentiality for thermoelectric applications. The large Seebeck coefficient originates from the modulation of the band gap achieved by the incorporation of BN atoms. This leads to high full ZT of ∼6 for the γ-graphyne-like BN sheet at room temperature. Our present study shows that these materials have huge potential for thermoelectricity. We hope that our report of a large value of ZT will motivate the experimentalists to characterize BN-doped graphyne systems.

ASSOCIATED CONTENT

Supporting Information

The Supporting Information is available free of charge at https://pubs.acs.org/doi/10.1021/acsomega.1c01538.

Structural coordinates of pristine γ-graphyne and BN-doped γ-graphyne systems; electronic part of the thermoelectric figure of merit (ZT_e) for pristine and BN doped γ-graphynes at different temperatures; and phonon band structure (PDF)

AUTHOR INFORMATION

Corresponding Authors

Utpal Sarkar − *Department of Physics, Assam University, Silchar 788011, India;* orcid.org/0000-0002-7677-7479; Email: utpalchemiitkgp@yahoo.com

Hatef Sadeghi − *Device Modelling Group, School of Engineering, University of Warwick, Coventry CV4 7AL, U.K.;* orcid.org/0000-0001-5398-8620; Email: hatef.sadeghi@warwick.ac.uk

Authors

Jyotirmoy Deb − *Department of Physics, Assam University, Silchar 788011, India;* orcid.org/0000-0002-1428-5137

Rajkumar Mondal − *Department of Physics, Assam University, Silchar 788011, India; Department of Physics, Nabadwip Vidyasagar College, Nabadwip, West Bengal 741302, India;* orcid.org/0000-0002-5237-5360

Complete contact information is available at: https://pubs.acs.org/10.1021/acsomega.1c01538

Notes

The authors declare no competing financial interest.

ACKNOWLEDGMENTS

J.D. thanks the Department of Science and Technology, New Delhi, for providing him DST-INSPIRE Fellowship. U.S. would like to thank the DBT-NECBH twinning project (ref. no. NECBH/2019-20/122), India, for financial assistance. H.S. thanks UKRI for funding (Future Leaders Fellowship number MR/S015329/2).

REFERENCES

(1) Nika, D. L.; Balandin, A. A. Two-dimensional phonon transport in graphene. *J. Phys.: Condens. Matter* **2012**, *24*, 233203.

(2) Bell, L. E. Cooling, heating, generating power, and recovering waste heat with thermoelectric systems. *Science* **2008**, *321*, 1457−1461.

(3) Page, A.; Van der Ven, A.; Poudeu, P. F. P.; Uher, C. Origins of phase separation in thermoelectric (Ti, Zr, Hf) NiSn half-Heusler alloys from first principles. *J. Mater. Chem. A* **2016**, *4*, 13949−13956.

(4) Majumdar, A. Thermoelectricity in semiconductor nanostructures. *Science* **2004**, *303*, 777−778.

(5) Hicks, L. D.; Dresselhaus, M. S. Effect of quantum-well structures on the thermoelectric figure of merit. *Phys. Rev. B: Condens. Matter Mater. Phys.* **1993**, *47*, 12727.

(6) Zuev, Y. M.; Chang, W.; Kim, P. Thermoelectric and magnetothermoelectric transport measurements of graphene. *Phys. Rev. Lett.* **2009**, *102*, 096807.

(7) Wei, P.; Bao, W.; Pu, Y.; Lau, C. N.; Shi, J. Anomalous thermoelectric transport of Dirac particles in graphene. *Phys. Rev. Lett.* **2009**, *102*, 166808.

(8) Sevinçli, H.; Cuniberti, G. Enhanced thermoelectric figure of merit in edge-disordered zigzag graphene nanoribbons. *Phys. Rev. B: Condens. Matter Mater. Phys.* **2010**, *81*, 113401.

(9) Sun, L.; Jiang, P. H.; Liu, H. J.; Fan, D. D.; Liang, J. H.; Wei, J.; Cheng, L.; Zhang, J.; Shi, J. Graphdiyne: A two-dimensional thermoelectric material with high figure of merit. *Carbon* **2015**, *90*, 255−259.

(10) Tan, X.; Shao, H.; Hu, T.; Liu, G.; Jiang, J.; Jiang, H. High thermoelectric performance in two-dimensional graphyne sheets predicted by first-principles calculations. *Phys. Chem. Chem. Phys.* **2015**, *17*, 22872−22881.

(11) Jiang, P. H.; Liu, H. J.; Cheng, L.; Fan, D. D.; Zhang, J.; Wei, J.; Liang, J. H.; Shi, J. Thermoelectric properties of γ-graphyne from first-principles calculations. *Carbon* **2017**, *113*, 108−113.

(12) Wang, X.-M.; Lu, S.-S. Thermoelectric transport in graphyne nanotubes. *J. Phys. Chem. C* **2013**, *117*, 19740−19745.

(13) Wang, X.-M.; Mo, D.-C.; Lu, S.-S. On the thermoelectric transport properties of graphyne by the first-principles method. *J. Chem. Phys.* **2013**, *138*, 204704.

(14) Novoselov, K. S.; Geim, A. K.; Morozov, S. V.; Jiang, D.; Zhang, Y.; Dubonos, S. V.; Grigorieva, I. V.; Firsov, A. A. Electric field effect in atomically thin carbon films. *Science* **2004**, *306*, 666−669.

(15) Neto, A. H. C.; Guinea, F.; Peres, N. M. R.; Novoselov, K. S.; Geim, A. K. The electronic properties of graphene. *Rev. Mod. Phys.* **2009**, *81*, 109.
(16) Morozov, S. V.; Novoselov, K. S.; Katsnelson, M. I.; Schedin, F.; Elias, D. C.; Jaszczak, J. A.; Geim, A. K. Giant intrinsic carrier mobilities in graphene and its bilayer. *Phys. Rev. Lett.* **2008**, *100*, 016602.
(17) Xu, Y.; Li, Z.; Duan, W. Thermal and thermoelectric properties of graphene. *Small* **2014**, *10*, 2182−2199.
(18) Ni, X.; Liang, G.; Wang, J.-S.; Li, B. Disorder enhances thermoelectric figure of merit in armchair graphane nanoribbons. *Appl. Phys. Lett.* **2009**, *95*, 192114.
(19) Ouyang, Y.; Guo, J. A theoretical study on thermoelectric properties of graphene nanoribbons. *Appl. Phys. Lett.* **2009**, *94*, 263107.
(20) Sevinçli, H.; Sevik, C.; Çağın, T.; Cuniberti, G. A bottom-up route to enhance thermoelectric figures of merit in graphene nanoribbons. *Sci. Rep.* **2013**, *3*, 1355.
(21) Mazzamuto, F.; Nguyen, V. H.; Apertet, Y.; Caër, C.; Chassat, C.; Saint-Martin, J.; Dollfus, P. Enhanced thermoelectric properties in graphene nanoribbons by resonant tunneling of electrons. *Phys. Rev. B: Condens. Matter Mater. Phys.* **2011**, *83*, 235426.
(22) Baughman, R. H.; Eckhardt, H.; Kertesz, M. Structure-property predictions for new planar forms of carbon: Layered phases containing sp^2 and sp atoms. *J. Chem. Phys.* **1987**, *87*, 6687−6699.
(23) Malko, D.; Neiss, C.; Viñes, F.; Görling, A. Competition for graphene: graphynes with direction-dependent dirac cones. *Phys. Rev. Lett.* **2012**, *108*, 086804.
(24) Narita, N.; Nagai, S.; Suzuki, S.; Nakao, K. Optimized geometries and electronic structures of graphyne and its family. *Phys. Rev. B: Condens. Matter Mater. Phys.* **1998**, *58*, 11009.
(25) Kang, J.; Li, J.; Wu, F.; Li, S.-S.; Xia, J.-B. Elastic, electronic, and optical properties of two-dimensional graphyne sheet. *J. Phys. Chem. C* **2011**, *115*, 20466−20470.
(26) Chen, J.; Xi, J.; Wang, D.; Shuai, Z. Carrier mobility in graphyne should be even larger than that in graphene: a theoretical prediction. *J. Phys. Chem. Lett.* **2013**, *4*, 1443−1448.
(27) Bhattacharya, B.; Sarkar, U. The effect of boron and nitrogen doping in electronic, magnetic, and optical properties of graphyne. *J. Phys. Chem. C* **2016**, *120*, 26793−26806.
(28) Bhattacharya, B.; Paul, D.; Sarkar, U. Electronic and optical properties of XN-ynes (X= B, Al, Ga): A first-principle study with many-body effects. *Appl. Surf. Sci.* **2019**, *495*, 143612.
(29) Bhattacharya, B.; Deb, J.; Sarkar, U. Boron-phosphorous doped graphyne: A near-infrared light absorber. *AIP Adv.* **2019**, *9*, 095031.
(30) Deb, J.; Bhattacharya, B.; Singh, N. B.; Sarkar, U. First principle study of adsorption of boron-halogenated system on pristine graphyne. *Struct. Chem.* **2016**, *27*, 1221−1227.
(31) Deb, J.; Paul, D.; Pegu, D.; Sarkar, U. Adsorption of hydrazoic acid on pristine graphyne sheet: a computational study. *Acta Phys.-Chim. Sin.* **2018**, *34*, 537−542.
(32) Bhattacharya, B.; Sarkar, U.; Seriani, N. Electronic properties of homo-and heterobilayer graphyne: The idea of a nanocapacitor. *J. Phys. Chem. C* **2016**, *120*, 26579−26587.
(33) He, J.; Ma, S. Y.; Zhou, P.; Zhang, C. X.; He, C.; Sun, L. Z. Magnetic properties of single transition-metal atom absorbed graphdiyne and graphyne sheet from DFT+ U calculations. *J. Phys. Chem. C* **2012**, *116*, 26313−26321.
(34) Li, Q.; Yang, C.; Wu, L.; Wang, H.; Cui, X. Converting benzene into γ-graphyne and its enhanced electrochemical oxygen evolution performance. *J. Mater. Chem. A* **2019**, *7*, 5981−5990.
(35) Singh, N. B.; Bhattacharya, B.; Sarkar, U. A first principle study of pristine and BN-doped graphyne family. *Struct. Chem.* **2014**, *25*, 1695−1710.
(36) Zhang, Y.; Yun, J.; Wang, K.; Chen, X.; Yang, Z.; Zhang, Z.; Yan, J.; Zhao, W. First-principle study of graphyne-like BN sheet: Electronic structure and optical properties. *Comput. Mater. Sci.* **2017**, *136*, 12−19.
(37) Tromer, R. M.; Freitas, A.; Felix, I. M.; Mortazavi, B.; Machado, L. D.; Azevedo, S.; Pereira, L. F. C. Electronic, Optical and Thermoelectric Properties of Boron-Doped Nitrogenated Holey Graphene. *Phys. Chem. Chem. Phys.* **2020**, *22*, 21147−21157.
(38) Bark, H.; Lee, W.; Lee, H. Correlation between Seebeck Coefficients and Electronic Structures of Nitrogen- or Boron-Doped Reduced Graphene Oxide via Thermally Activated Carrier Transport. *J. Mater. Chem. A* **2018**, *6*, 15577−15584.
(39) Dong, C.; Meng, B.; Liu, J.; Wang, L. B ← N Unit Enables N-Doping of Conjugated Polymers for Thermoelectric Application. *ACS Appl. Mater. Interfaces* **2020**, *12*, 10428−10433.
(40) Soler, J. M.; Artacho, E.; Gale, J. D.; García, A.; Junquera, J.; Ordejón, P.; Sánchez-Portal, D. The SIESTA method for ab initio order-N materials simulation. *J. Phys.: Condens. Matter* **2002**, *14*, 2745.
(41) Perdew, J. P.; Burke, K.; Ernzerhof, M. Generalized gradient approximation made simple. *Phys. Rev. Lett.* **1996**, *77*, 3865.
(42) Troullier, N.; Martins, J. A straightforward method for generating soft transferable pseudopotentials. *Solid State Commun.* **1990**, *74*, 613−616.
(43) Ferrer, J.; Lambert, C. J.; García-Suárez, V. M.; Manrique, D. Z.; Visontai, D.; Oroszlany, L.; Rodríguez-Ferradás, R.; Grace, I.; Bailey, S. W. D.; Gillemot, K.; Sadeghi, H.; Algharagholy, L. A. GOLLUM: a next-generation simulation tool for electron, thermal and spin transport. *New J. Phys.* **2014**, *16*, 093029.
(44) Sadeghi, H. Theory of electron, phonon and spin transport in nanoscale quantum devices. *Nanotechnology* **2018**, *29*, 373001.
(45) Sadeghi, H.; Sangtarash, S.; Lambert, C. J. Oligoyne Molecular Junctions for Efficient Room Temperature Thermoelectric Power Generation. *Nano Lett.* **2015**, *15*, 7467−7472.
(46) Puigdollers, A. R.; Alonso, G.; Gamallo, P. First-principles study of structural, elastic and electronic properties of α-, β-and γ-graphyne. *Carbon* **2016**, *96*, 879−887.
(47) Bhattacharya, B.; Seriani, N.; Sarkar, U. Raman and IR signature of pristine and BN-doped γ-graphyne from first-principle. *Carbon* **2019**, *141*, 652−662.
(48) Cheng, L.; Liu, H. J.; Zhang, J.; Wei, J.; Liang, J. H.; Shi, J.; Tang, X. F. Effects of van der Waals interactions and quasiparticle corrections on the electronic and transport properties of Bi_2Te_3. *Phys. Rev. B: Condens. Matter Mater. Phys.* **2014**, *90*, 085118.
(49) Johnson, V. A.; Lark-Horovitz, K. Theory of Thermoelectric Power in Semiconductors with Applications to Germanium. *Phys. Rev.* **1953**, *92*, 226−232.
(50) Reshak, A. H.; Khan, S. A.; Auluck, S. Thermoelectric properties of a single graphene sheet and its derivatives. *J. Mater. Chem. C* **2014**, *2*, 2346−2352.
(51) Manoharan, K.; Subramanian, V. Exploring multifunctional applications of hexagonal boron arsenide sheet: a DFT study. *ACS Omega* **2018**, *3*, 9533−9543.
(52) Sun, L.; Jiang, P. H.; Liu, H. J.; Fan, D. D.; Liang, J. H.; Wei, J.; Cheng, L.; Zhang, J.; Shi, J. Graphdiyne: A two-dimensional thermoelectric material with high figure of merit. *Carbon* **2015**, *90*, 255−259.
(53) Fei, R.; Faghaninia, A.; Soklaski, R.; Yan, J.-A.; Lo, C.; Yang, L. Enhanced thermoelectric efficiency via orthogonal electrical and thermal conductances in phosphorene. *Nano Lett.* **2014**, *14*, 6393−6399.
(54) Kumar, S.; Schwingenschlögl, U. Thermoelectric response of bulk and monolayer $MoSe_2$ and WSe_2. *Chem. Mater.* **2015**, *27*, 1278−1284.
(55) Cheng, L.; Liu, H.; Tan, X.; Zhang, J.; Wei, J.; Lv, H.; Shi, J.; Tang, X. Thermoelectric properties of a monolayer bismuth. *J. Phys. Chem. C* **2014**, *118*, 904−910.
(56) Yun, W. S.; Lee, J. D. Exploring a Novel Atomic Layer with Extremely Low Lattice Thermal Conductivity: $ZnPSe_3$ and Its Thermoelectrics. *J. Phys. Chem. C* **2018**, *122*, 27917−27924.
(57) Lin, C.; Cheng, W.; Chai, G.; Zhang, H. Thermoelectric Properties of Two-Dimensional Selenene and Tellurene from Group-VI Elements. *Phys. Chem. Chem. Phys.* **2018**, *20*, 24250−24256.

https://doi.org/10.1021/acsomega.1c01538
ACS Omega 2021, 6, 20149−20157

(58) Yumnam, G.; Pandey, T.; Singh, A. K. High temperature thermoelectric properties of Zr and Hf based transition metal dichalcogenides: A first principles study. *J. Chem. Phys.* **2015**, *143*, 234704.
(59) Sadeghi, H. Theory of Electron, Phonon and Spin Transport in Nanoscale Quantum Devices. *Nanotechnology* **2018**, *29*, 373001.
(60) Bhattacharya, B.; Singh, N. B.; Sarkar, U. Tuning the Magnetic Property of Vacancy-Defected Graphyne by Transition Metal Absorption. *AIP Conf. Proc.* **2015**, *1665*, 050066.
(61) Cui, C.; Ouyang, T.; Tang, C.; He, C.; Li, J.; Zhang, C.; Zhong, J. Bayesian Optimization-Based Design of Defect Gamma-Graphyne Nanoribbons with High Thermoelectric Conversion Efficiency. *Carbon* **2021**, *176*, 52−60.
(62) Cui, X.; Ouyang, T.; Li, J.; He, C.; Tang, C.; Zhong, J. Enhancing the Thermoelectric Performance of Gamma-Graphyne Nanoribbons by Introducing Edge Disorder. *Phys. Chem. Chem. Phys.* **2018**, *20*, 7173−7179.
(63) Liang, J.; Liu, H.; Fan, D.; Jiang, P. Large-Scale Calculations of Thermoelectric Transport Coefficients: A Case Study Of γ-Graphyne with Point Defects. *J. Phys.: Condens. Matter* **2017**, *29*, 455901.

https://doi.org/10.1021/acsomega.1c01538
ACS Omega 2021, 6, 20149−20157